ISPRS Journal of Photogrammetry and Remote Sensing 66 (2011) 2–16

Contents lists available at ScienceDirect

ISPRS Journal of Photogrammetry and Remote Sensing

journal homepage: www.elsevier.com/locate/isprsjprs

Object-based image analysis through nonlinear scale-space filtering

Angelos Tzotsos [a,*], Konstantinos Karantzalos [a,b], Demetre Argialas [a]

[a] National Technical University of Athens, Remote Sensing Laboratory, Athens, Greece

[b] Ecole Centrale de Paris, Laboratoire de Mathematiques Appliquees aux Systemes, Chatenay-Malabry, France

ARTICLE INFO

Article history:
Received 31 July 2009
Received in revised form
27 May 2010
Accepted 14 July 2010
Available online 17 September 2010

Keywords:
Automation
Analysis
Simplification
Segmentation
Classification

ABSTRACT

In this research, an object-oriented image classification framework was developed which incorporates nonlinear scale-space filtering into the multi-scale segmentation and classification procedures. Morphological levelings, which possess a number of desired spatial and spectral properties, were associated with anisotropically diffused markers towards the construction of nonlinear scale spaces. Image objects were computed at various scales and were connected to a kernel-based learning machine for the classification of various earth-observation data from both active and passive remote sensing sensors. Unlike previous object-based image analysis approaches, the scale hierarchy is implicitly derived from scale-space representation properties. The developed approach does not require the tuning of any parameter—of those which control the multi-scale segmentation and object extraction procedure, like shape, color, texture, etc. The developed object-oriented image classification framework was applied on a number of remote sensing data from different airborne and spaceborne sensors including SAR images, high and very high resolution panchromatic and multispectral aerial and satellite datasets. The very promising experimental results along with the performed qualitative and quantitative evaluation demonstrate the potential of the proposed approach.

1. Introduction

Along with the gradual availability of earth-observation data with higher spatial and spectral resolution, research efforts in classifying remote sensing data have been shifting in the last decade from pixel-based to object-based approaches. Assigning land cover classes to individual pixels can be intuitively proper and functional for low-resolution data. However, this is not the case for the emerging applications which arise from the continuously improving remote sensing sensors (Aplin and Smith, 2008; Blaschke et al., 2008; Blaschke, 2010). This is mostly because, at higher resolutions, it is a connected group of pixels that is likely to be associated with a land cover class and not just an individual pixel.

In addition, the earth surface exhibits various regular and irregular structures which are represented with a certain spatial heterogeneity in images. This heterogeneity appears with variations in intensity, scale and texture. Several important aspects of earth-observation data cannot be analyzed based on pixel information, but can only be exploited based on contextual information and the topologic relations of the objects of interest (Argialas and Harlow, 1990; Liu et al., 2008) through a multi-scale image analysis (Blaschke and Hay, 2001; Hay et al., 2002; Hall and Hay, 2003; Benz et al., 2004; Stewart et al., 2004; Jimenez et al., 2005; Duarte Carvajalino et al., 2008; Ouma et al., 2008). Starting with the observed spatial heterogeneity and variability, meaningful spatial aggregations (objects) can be formed at certain image scales configuring a relationship between ground objects and image objects. With such an object-based multi-scale analysis, which is based on certain hierarchically structured rules, the relationships between the different scales of the spatial entities are being described.

The semantic objects of an image do not belong to a single but to various spatial scales. The use of scale-space image representations is thus of fundamental importance for a number of image analysis and computer vision tasks. It dates back to 1960s and was first introduced by Iijima (Weickert et al., 1999). Following the ideas of Witkin (1983), Koenderink (1984) and Lindeberg (1994), many methods have been introduced to derive linear scale spaces and respectively many isotropic multi-scale operators have been developed. Either through Gaussian filtering or through isotropic multi-resolution analysis (e.g. by down-sampling the initial data), all linear scale-space approaches present the same important drawback: image edges are blurred and new non-semantic objects may appear at coarse filtering scales (Witkin, 1983; Paragios et al., 2005; Ouma et al., 2008). Under a hierarchical multi-scale segmentation or an object-based classification framework,

* Corresponding address: Heroon Polytechniou 9, Zographos, 15780, Greece. Tel.: +30 210 7722684; fax: +30 210 7722594.
E-mail addresses: tzotsos@gmai1.com (A. Tzotsos), konstantinos.karantza1os@ecp.fr (K. Karantzalos), argia1as@centra1.ntua.gr (D. Argialas).

0924-2716/$ – see front matter
doi:10.1016/j.isprsjprs.2010.07.001

the thematic information to be extracted is directly related with the primitive image objects computed at every segmentation scale. The better these primitive objects represent real-world entities, the better they can describe the semantics of the image (Hay and Castilla, 2006; Blaschke et al., 2008; Hofmann et al., 2008). Therefore, the selection of the appropriate approach for constructing the multi-scale image and the hierarchical object representation is of great importance.

The motivation, here, is to embed into an object-based processing scheme an advanced scale-space formulation, which possesses suitable qualitative properties desired in image analysis and remote sensing. The introduced image classification framework incorporates advanced morphological scale-space filtering and therefore enforces the multi-scale segmentation and class separation procedures to be constrained by hierarchically simplified image representations. Morphological levelings, a kind of advanced self-dual morphological operators, were selected possessing a number of desired spatial and spectral properties (Meyer and Maragos, 2000; Meyer, 2004; Karantzalos et al., 2007) and were associated with anisotropically diffused markers. Based on these advanced multi-scale image representations, image objects were computed at various segmentation scales and were connected to a kernel-based learning machine for the classification of various earth-observation data from both active and passive remote sensing sensors.

Previous object-based image analysis approaches (Baatz and Schape, 2000; Hay et al., 2002; Benz et al., 2004; Blaschke et al., 2004; Carleer et al., 2005; Tzotsos and Argialas, 2006; Tzotsos et al., 2008; Ouma et al., 2008; Dragut et al., 2009; Zhou et al., 2009) require the tuning of parameters (such as shape, color, segmentation scale, texture, etc.) that define the multi-scale object representation. By contrast, in our approach, the scale hierarchy is implicitly derived from scale-space representation principles. Furthermore, the developed framework does not incorporate (i) any linear scale-space filtering (like in Blaschke and Hay, 2001; Hay et al., 2003, 2002; Stewart et al., 2004) or (ii) any multi-resolution image representation by down-sampling the image at different spatial resolutions (like in Hall and Hay, 2003). Such a process actually performs in a similar way with the isotropic filtering, possessing the same qualitative drawbacks. In the proposed approach, advanced morphological scale-space representations have been embedded in the object-based image analysis framework and thus, the construction of multi-scale hierarchical object representations was adequately constrained by a refined edge-preserving geometric image simplification (Fig. 1). Last but not least, unlike other research efforts which exploited the use of anisotropic diffusion for pixel-based remote sensing data classification (Lennon et al., 2002; Camps-valls and Bruzzone, 2005; Plaza et al., 2009), the developed methodology introduces the use of anisotropic morphological levelings (Karantzalos et al., 2007; Karantzalos, 2008) under an object-oriented classification scheme.

The remainder of the paper is structured as follows. In Section 2, the related work on the use of scale-space techniques and object-based classification schemes for remote sensing applications is briefly described. The developed object-based classification framework is detailed in Section 3, along with a description and detailed analysis of its different processing steps. Experimental results, the performed quantitative evaluation and the discussion of results are given in Section 4. Finally, conclusions and perspectives for future work are in Section 5.

2. Related work

2.1. Scale-space representations for remote sensing image analysis

There are linear and nonlinear scale-space representations. Since linear scale-space approaches, by acting isotropically in the image domain, delocalize and blur image edges, nonlinear operators and nonlinear scale spaces have been studied and applied in various image processing and computer vision applications. Following the pioneering work of Perona and Malik (1990), there has been a flurry of activity in partial differential equation approaches and anisotropic diffusion filtering techniques (Weickert, 1998). For remote sensing applications, a number of anisotropic diffusion schemes have been proposed and applied to aerial and satellite datasets (Lennon et al., 2002; Camps-valls and Bruzzone, 2005; Karantzalos and Argialas, 2006; Duarte-Carvajalino et al., 2007; Ouma et al., 2008; Plaza et al., 2009), combined, in most cases, with pixel-based classification techniques. These scale-space formulations were based either on diffusions during which the average luminance value is preserved or on geometrically driven approaches formulated under a variational framework. Although these formulations may reduce the problems of isotropic filtering, they do not eliminate them completely: spurious extrema and important intensity shifts may still appear (Meyer and Maragos, 2000; Karantzalos et al., 2007).

Another approach to produce nonlinear scale spaces is through mathematical morphology and, in particular, with morphological levelings, which have been introduced by Meyer (1998) and further studied by Matheron (1997) and Serra (2000). Morphological levelings overcome the drawback of spurious extrema or important intensity shifts and possess a number of desired properties for the construction of advanced scale-space representations. Levelings, which are a general class of self-dual morphological operators, do not displace contours through scales and are characterized by a number of desirable properties for the construction of nonlinear scale-space representations. They satisfy the following spatial and spectral properties/principles (Meyer and Maragos, 2000; Meyer, 2004; Karantzalos et al., 2007):

- invariance by spatial translation,
- isotropy, invariance by rotation,
- invariance to a change of illumination,
- the causality principle,
- the maximum principle, excluding the extreme case where the image is completely flat.

In addition, levelings

- do not produce new extrema at larger filtering scales,
- enlarge smooth zones,
- they also create new smooth zones,
- they are particularly robust (strong morphological filters),
- they do not displace edges.

Following the definitions from Meyer (2004) and Karantzalos et al. (2007), by comparing the values of neighboring pixels in the image domain, levelings are a particular class of images with fewer contours than a given image f. One can define a function g as a leveling of another function f if and only if the following inequality holds:

$$f \wedge \delta g \leq g \leq f \vee \varepsilon g, \tag{1}$$

where δ is an extensive operator ($\delta g \geq g$) and ε an anti-extensive one ($\varepsilon g \leq g$).

For the construction of levelings, a class of functions h is defined, which separates function g from the reference function f. This type of function is known as a marker function (Meyer and Maragos, 2000) and can be defined with the following formulation $g \wedge f \leq h \leq g \vee f$. Algorithmically, one can interpret the above equation and construct levelings with the following pseudo-code: in cases where $h < f$, replace the values of h with $f \wedge \delta h$ and in cases where $\{h > f\}$, replace the values of h with $f \vee \varepsilon h$. Equally and in a single parallel step, we have

$$h = (f \wedge \delta h) \vee \varepsilon h. \tag{2}$$


(a) Initial image.


(b) Crop.

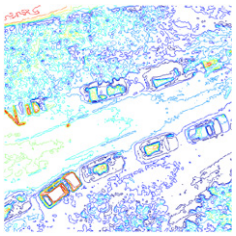
(c) Contours.

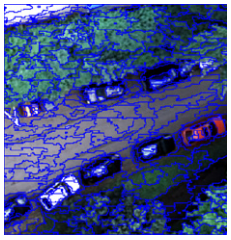
(d) Segments.


(e) MR, Sc: 0.8.


(f) Gauss, Sc: 2.


(g) ALM, Sc: 50.


(h) AML, Sc: 50.


(i) MR, Sc: 0.4.


(j) Gauss, Sc: 7.


(k) ALM, Sc: 500.


(l) AML, Sc: 500.

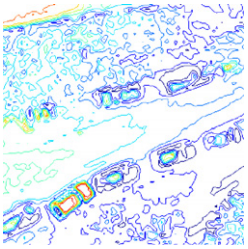
(m) Contours MR.

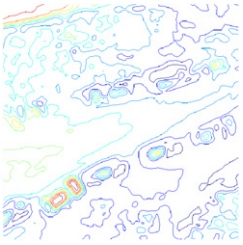
(n) Contours Gauss.

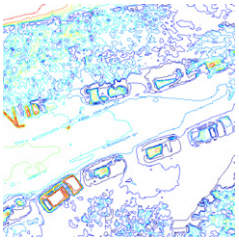
(o) Contours ALM.

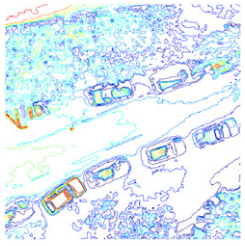
(p) Contours AML.

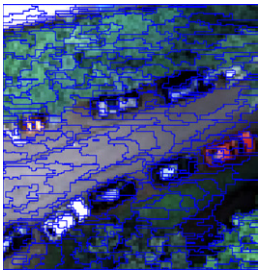
(q) Segments MR.

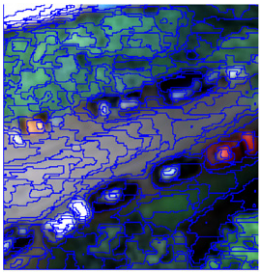
(r) Segments Gauss.

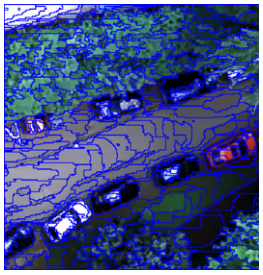
(s) Segments ALM.

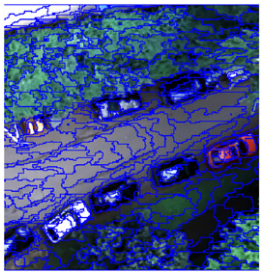
(t) Segments AML.

Fig. 1. Comparing the scale-space representation of linear and nonlinear techniques. Two scales from each technique are presented, along with the corresponding image contours (isophotes) (c, m, n, o, p) and the coarser scale (i, j, k, l) segments (q, r, s, t). For the multi-resolution (MR) approach, the scales (Sc) of 0.8 and 0.4 are shown computed by a down-sampling of the initial image. For the Gaussian smoothing, the scales (standard deviation values) of 2 and 7 are presented and for the nonlinear approaches ALM and AML the scales (iterations) of 50 and 500. One can observe that both nonlinear approaches (AML, ALM) do not blur image edges, do not produce new extrema and more effectively and accurately preserve image contours.

The algorithm is repeated until the above equation has been satisfied everywhere. This convergence is certain since the replacements on the values of h are pointwise monotonic. Hence, levelings can be considered as transformations $\Lambda(f, h)$ where a marker h is transformed to a function g, which is a leveling of the reference signal f, where $\{h < f\}$, h is increased as little as possible until a flat zone is created or function g reaches the reference function f and where $\{h > f\}$, h is decreased as little as possible

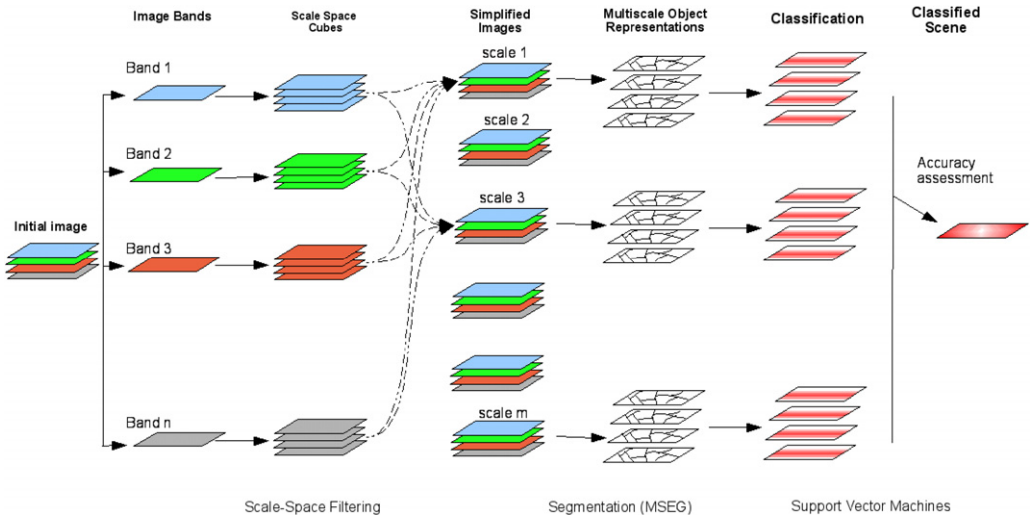

Fig. 2. The developed framework embeds nonlinear scale-space filtering into the object-based image classification procedure.

(a) Original image. (b) AML, scale: 100. (c) AML, scale: 500.

Fig. 3. AML filtering results on DMC aerial multispectral image with 5 cm pixel-size (Intergraph Corp.©).

until a flat zone is created or function g reaches the reference function f. This makes function g to be flat on $\{g < f\}$ and $\{g > f\}$ and the procedure continues until convergence.

Different types of levelings can be constructed based on different types of extensive δ and anti-extensive ε operators. Based on a family of extensive dilations δ_i and the corresponding family of adjunct erosions ε_i, where $\delta_i < \delta_j$ and $\varepsilon_i > \varepsilon_j$ for $i > j$, multi-scale levelings (a hierarchy of levelings) can be constructed (Meyer and Maragos, 2000). Multi-scale levelings can also be constructed when the reference function f is associated with a series of marker functions $\{h_1, h_2, \ldots, h_n\}$. The constructed levelings are respectively,

$$g_1 = f, \qquad g_2 = \Lambda(f, h_1), \\ g_3 = \Lambda(f, h_2), \ldots, g_{n+1} = \Lambda(f, h_n). \tag{3}$$

Thus, a series of simpler and simpler images, with fewer and fewer smooth zones, are produced.

2.2. Object-based image analysis

Instead of classifying individual pixels into discrete land cover classes, object-based classification approaches construct a hierarchical object representation of an image and the classifier is responsible for associating them with a land cover class. Therefore, it is not just the spectral signature of each pixel, but the statistical, geometric and topological characteristics of each object that play a key role during classification.

The commercial availability of such an object-based image analysis software (Baatz and Schape, 2000) enabled the accomplishment of several studies for various engineering and environmental remote sensing applications (Benz et al., 2004; Zhou et al., 2009; Dragut et al., 2009, and references therein). To this end, during the last decade, the challenge was to construct an efficient object representation through certain multi-scale (region merging or other) segmentation techniques (Blaschke et al., 2004; Carleer et al., 2005; Jimenez et al., 2005; Neubert et al., 2006; Tzotsos and Argialas, 2006), which partition the image on several regions/objects based on the spectral homogeneity in a local neighborhood. In addition to the spectral homogeneity criterion, shape parameters are used to define geometric properties that the segmentation algorithm must take into account when computing the overall homogeneity (scale parameter) of each image object during the search for optimal merges. A texture optimization procedure was introduced for the MSEG algorithm (Tzotsos et al., 2008) integrating grey level co-occurrence matrices and introducing an object-based cost measure for texture homogeneity as an additional parameter to the segmentation procedure. Such an integration of spatial and spectral information can produce a multi-scale object representation but only through an iterative and exhaustive tuning (based on trial and error investigation) of certain parameters, like shape, scale, texture, etc. (Baatz and Schape, 2000; Benz et al., 2004; Blaschke et al., 2004; Carleer et al., 2005; Hay et al., 2005; Tzotsos and Argialas, 2006; Ouma et al., 2008; Dragut et al., 2009; Zhou et al., 2009).

Other research efforts were based on the construction of linear scale spaces for the multi-scale analysis of several landscape

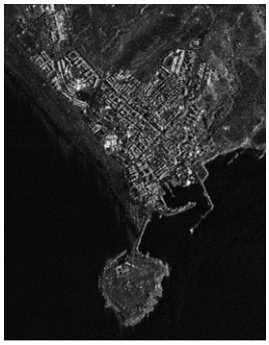

(a) Original image.

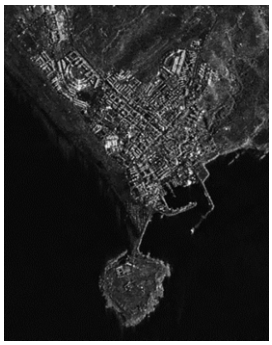

(b) AML, scale: 100.

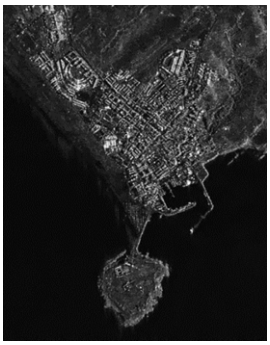

(c) AML, scale: 500.

(d) Original image.

(e) AML, scale: 100.

(f) AML, scale: 500.

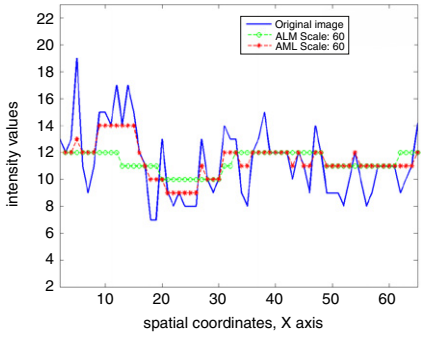

(g) ALM and AML at scale 60.

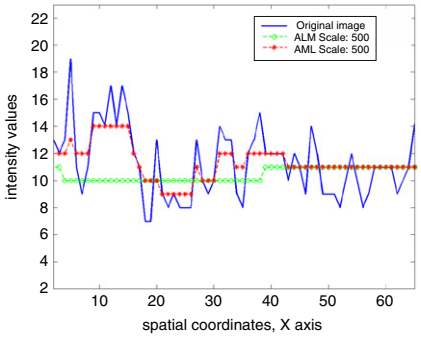

(h) ALM and AML at scale 500.

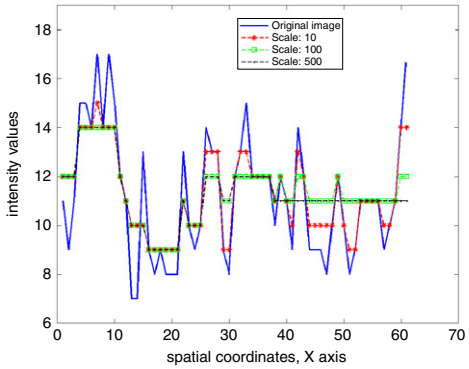

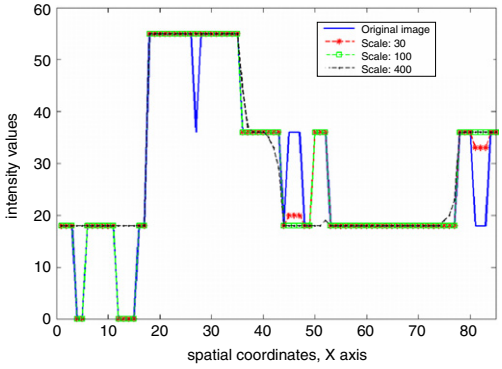

(i) Spatial cross sections at different AML scales.

Fig. 4. Applying the ALM and AML nonlinear scale spaces to a TerraSAR-X (DLR©) dataset (3 m ground resolution, StripMap mode, polarisation HH). At all scales the AML simplifies the initial image and stays closer to the initial intensity values.

structures (Blaschke and Hay, 2001; Hay et al., 2003, 2002; Stewart et al., 2004) or on the construction of multi-scale representations through object-specific analysis and up-scaling, through the computation of a number of coarse and fine scales by sampling the initial image (Hall and Hay, 2003).

The object-based classification framework developed here is based on (i) the construction of advanced morphological scale-space representations (Fig. 1) and (ii) an advanced kernel classifier, the Support Vector Machine (SVM). SVM (Vapnik, 1998; Theodoridis and Koutroumbas, 2003) is a state-of-the-art machine

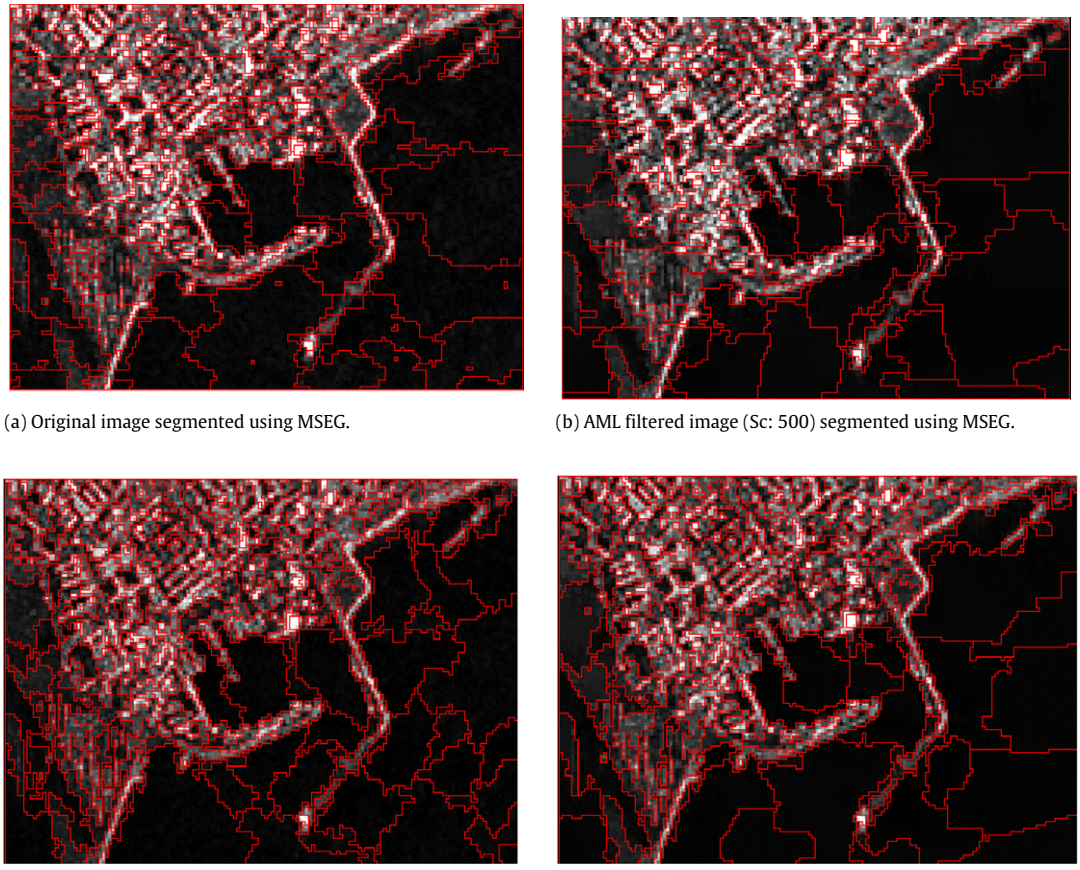

(a) Original image segmented using MSEG.

(b) AML filtered image (Sc: 500) segmented using MSEG.

(c) Original image segmented using eCognition.

(d) AML filtered image (Sc: 500) segmented using eCognition.

Fig. 5. TerraSAR-X (DLR©) segmentation results with and without the AML filtering using the MSEG and the eCognition software.

learning methodology that can be used for pattern classification and has proven to be very successful in pixel-based remote sensing applications (Huang et al., 2002; Mercier and Lennon, 2003; Foody and Mathur, 2004; Melgani and Bruzzone, 2004). Recently, an object-based image classification scheme was proposed using support vector machines (Tzotsos and Argialas, 2008).

3. Methodology

The developed object-based framework is integrating certain computer vision and machine learning methods for performing common object-based image analysis (OBIA) tasks, such as image segmentation, object hierarchy representation, classification, etc. This section is divided into three sub-sections which describe the three major components of the framework: scale-space filtering, image segmentation and kernel-based object classification. An overview of the developed approach is shown in Fig. 2. Before going into a detailed account of each of the three sections, a general presentation of the developed methodology is presented.

The proposed algorithm was designed in such a way that can take as an input any type of remote sensing imagery (Multispectral, Panchromatic, Radar, Hyperspectral, etc.). Every initial image is decomposed into its n separate bands in order to achieve the proper nonlinear filtering, depending on the scale parameter of the scale-space filter. For each band, a scale-space representation is created based on anisotropic morphological leveling (AML) formulation. Each scale-space cube is a 3D representation of the initial band at m successive filtering scales $(1, 2, 3, \ldots, m)$. From such a band-oriented representation, a scale-oriented one is constructed by merging bands of the same filtering scale. Thus, a series of m simplified images (of m successive filtering scales) is constructed, from which the multi-scale object representation will be derived.

A multi-scale region merging segmentation algorithm is then applied to each simplified image. During this procedure, the tuning of the standard segmentation parameters is of less importance, and only the scale parameter of the merging plays a key role. In contrast with most OBIA implementations, the size and shape of objects are constrained primarily by the morphological scale-space filtering. In Fig. 1 it can be observed that for the same segmentation parameters, different segment sizes are produced, with different shape each time. The segmentation algorithm is applied to each simplified image, without the need of tuning the standard parameters (shape, color, texture, etc.). The multilevel object representation is derived only using the segmentation scale parameter. Consequently, the final object hierarchy is dependent on the filtering scale and segmentation scale parameters.

The final step of the algorithm includes the definition of the class hierarchy, according to the semantics of the image, and the classification, which is performed by a support vector machine classifier using training samples for each class. For each level of objects created from the segmentation step and for all image filtering scales, a machine learning procedure is executed, providing object classifications of equal number. Finally, an accuracy assessment step is performed and the optimal classification result is selected.

3.1. Anisotropic morphological levelings

As in many digital remote sensing applications and methods, the first step in the developed approach is a low-level preprocessing of the original image. This initial filtering serves the purpose of removing noise, as well as simplifying the complexity

(a) Original image segmented using MSEG.

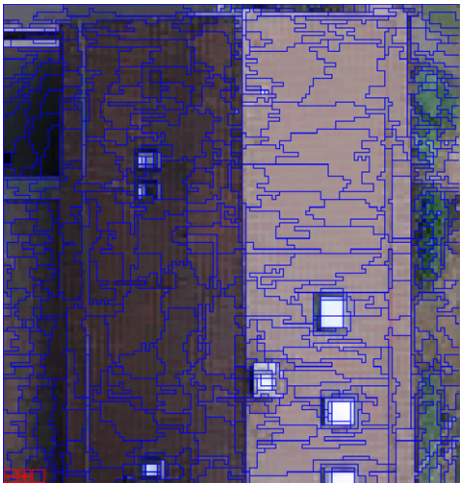

(b) AML filtered image (Sc: 1000) segmented using MSEG.

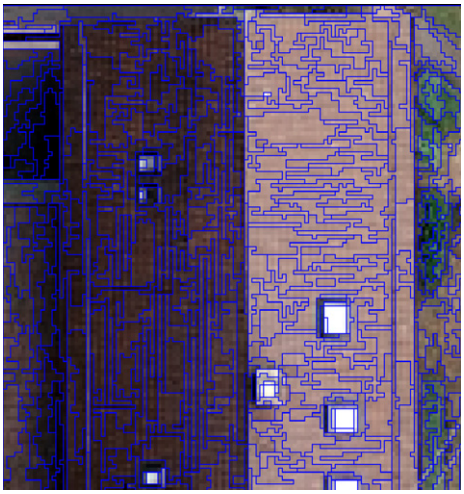

(c) Original image segmented using eCognition.

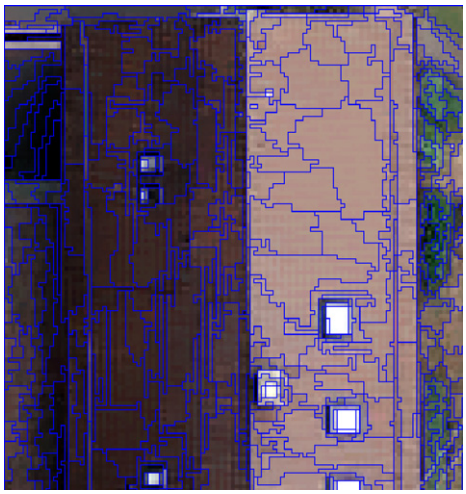

(d) AML filtered image (Sc: 1000) segmented using eCognition.

Fig. 6. Segmentation tests as performed on the DMC (Intergraph Corp.©) aerial image, with and without the application of nonlinear filtering.

of the information included in the original data. Especially in high spatial resolution remote sensing imagery, it is of great importance to reduce the heterogeneity of the original dataset in order to achieve better medium (segmentation) and high-level (classification) results. Image semantic objects tend to incorporate great value of spectral heterogeneity as the resolution gets higher with the recent available sensors. For example, in Fig. 3 an ultra-high spatial resolution image (5 cm pixel size) is presented acquired from an aerial multispectral scanner. One can observe the tiles on the roof of the building, the road marking signs and the fine texture of the rooftop material. It is obvious that this kind of detail cannot be addressed properly either through pixel-based procedures or through a simple OBIA scheme.

Therefore, nonlinear scale-space filtering was selected to be the first step towards properly simplifying the initial image, towards addressing the usual over-segmentation and misclassification problems. As stated previously, state-of-the-art filtering methods have moved away from linear models and tend to preserve the edge information like anisotropic diffusion (ADF). Morphological levelings are another powerful tool for obtaining scale-space information (Meyer and Maragos, 2000; Karantzalos and Argialas, 2006). A combination of morphological levelings with anisotropic markers, known as anisotropic morphological levelings (AML), have given better results, by possessing the ability for image simplification and at the same time by preserving important image properties (Karantzalos and Argialas, 2006; Karantzalos et al., 2007) (see Section 2.1).

In this study, an AML implementation has been incorporated as a pre-processing tool for object-based image analysis. Its native multi-scale representation ability was exploited along with the use of a multi-scale segmentation method to derive better image primitive objects, and thus better classification results. The AML filtering was applied to every single band of the original data. At each iteration, anisotropic markers were constructed based on the formulations of Alvarez et al. (1992). The greater the number of filtering scales used, the stronger the simplification since an equal number of diffusions are performed in the original data in order to provide the markers for the reconstruction of the leveling.

In the following sections, results from the use of AML filtering will be presented as well as its contribution to the overall developed approach for a variety of remote sensing data.

3.2. Multi-scale segmentation

For the multi-scale segmentation procedure, the MSEG algorithm was employed for providing the primitive image objects at

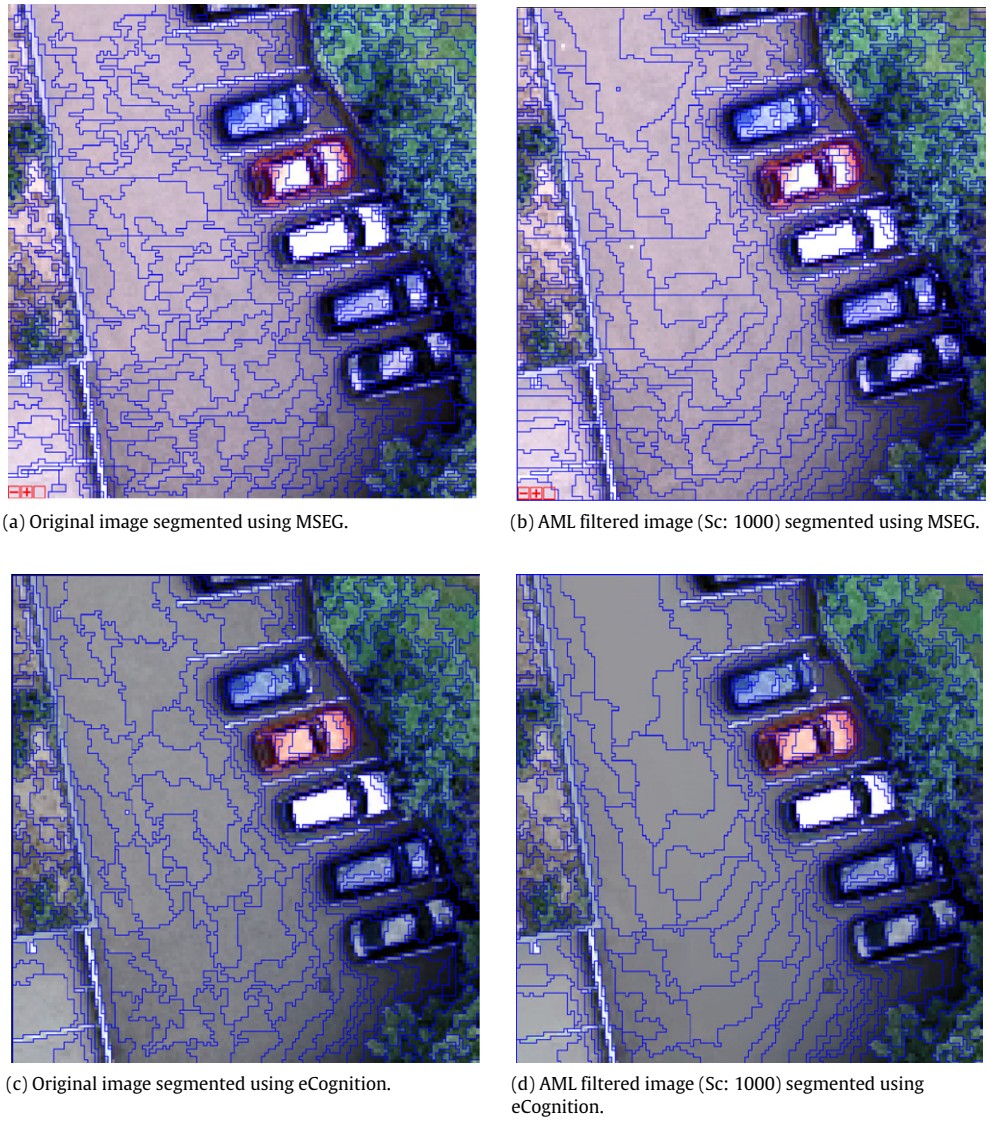

(a) Original image segmented using MSEG.

(b) AML filtered image (Sc: 1000) segmented using MSEG.

(c) Original image segmented using eCognition.

(d) AML filtered image (Sc: 1000) segmented using eCognition.

Fig. 7. Segmentation tests as performed on the DMC (Intergraph Corp.©) aerial image, with and without the application of nonlinear filtering.

different scale parameters. MSEG is a region-based multi-scale segmentation algorithm recently developed for object-oriented image analysis (Tzotsos and Argialas, 2006). It can be described as a region merging procedure, starting from a pixel representation and creating objects through continuous pair-wise object fusions, executed in iterations, called *passes* of the algorithm. For each pass, every object is evaluated in relation with its neighboring objects towards the optimal pair of objects adequate for fusion. In every pass, an image object can be merged only once, aiming at a balanced object growth.

In order to achieve reproducibility of results, a heuristic procedure was introduced, called starting point estimation (SPE). Using image statistics and color-space transformations, the image is partitioned in tiles and then starting points are computed for each tile (Tzotsos and Argialas, 2006). These points are not used as seeds, but are used to determine the order in which object merging evaluation will be performed. In this way, MSEG produces exactly the same result for the same parameters and the same initial image.

Like many other region-based segmentation algorithms (Pal and Pal, 1993; Baatz and Schape, 2000), the MSEG algorithm defines a cost function for each object merge and then implements various optimization techniques to minimize this cost. The cost function is implemented using the measure of homogeneity (color and shape) in the same way with other approaches (Baatz and Schape, 2000). The threshold of the allowed merging cost for the segmentation procedure is called scale parameter since it implicitly dictates the area growth of the image objects. In order to achieve a multi-scale object representation, several scale parameters must be defined during several executions of the segmentation algorithm. For the integrity of the topological relations of the objects, a set of cross-level constraints can be activated (Tzotsos and Argialas, 2006).

Given that the goal was to design a generic processing framework, several filtering and segmentation scales were examined and validated through quantitative and qualitative evaluation based on ground truth data. In particular, a sensitivity analysis was more than important in order to demonstrate that different types of remote sensing imagery respond differently to the same filtering and segmentation methods and, therefore, require different parameter settings for most OBIA procedures. For example, a 32-bit LiDAR dataset is segmented into smaller objects than an 8-bit multispectral image at the same scale parameter due to different radiometry, magnitude of edges, number of bands, etc.

A novelty of the developed segmentation process is that, by employing an elegant scale-space filtering, the tuning of the region-merging parameters is of less importance to the final segmentation result. There was no need for an exhaustive manual

(a) Original image zoom.

(b) AML, scale: 1000.

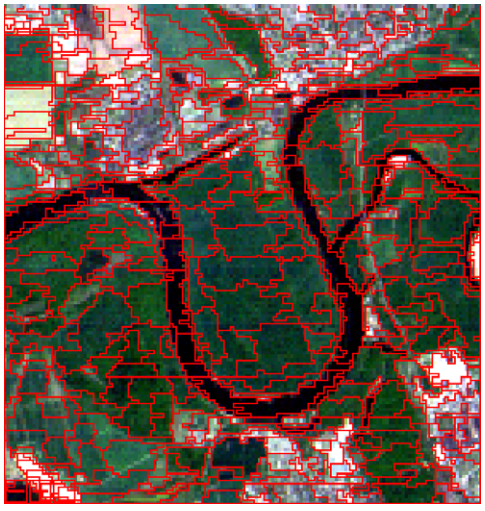

(c) Original image segmented using MSEG.

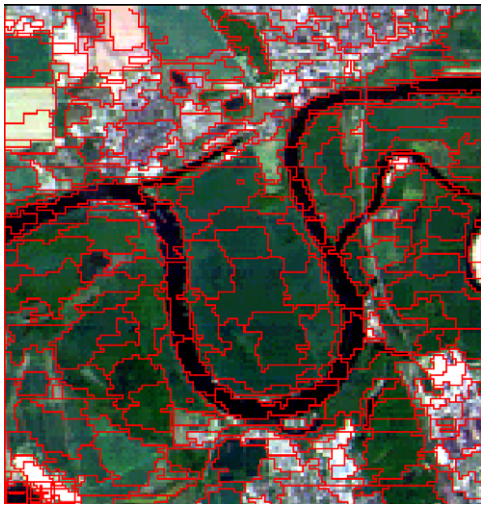

(d) AML filtered image (Sc: 1000) segmented using MSEG.

Fig. 8. A segmentation test as performed on a Landsat TM image, with and without the application of nonlinear filtering.

search to obtain the best parameter settings for multilevel segmentation. It is the scale-space filtering that primarily constrained the construction of the multi-scale object representation and not the region-merging procedure. A sensitivity analysis was performed to demonstrate this concept and it is discussed in the evaluation section below (Fig. 10, Section 4.3).

Using nonlinear scale-space filtering before segmentation leads to improvements as shown in Fig. 1. To further demonstrate this, having all parameters (except scale parameter) set to their default values during testing, several segmentation tests were performed on the initial images, as well as on the filtered images. Furthermore, tests were performed using the Baatz and Shape's segmentation algorithm producing improved results. The improved segmentation results can be implicitly proved by the increase of classification accuracy, when using the same segmentation parameters for the same image, the same class samples and the same classification parameters. Class samples were initially provided as external vector files and then a percentage of overlap between samples and objects was computed in order to select the sample objects for training.

3.3. Support vector machines

For the developed approach, the SVM classifier by Tzotsos and Argialas (2008) was employed. After image segmentation, image objects were extracted and object properties were computed forming the feature space of the classification problem. The computed properties are bound to each object by a unique identifier within the object hierarchy of the image. Some of the objects were selected as samples and their properties formed a training set for the SVM.

In general, the SVM seeks to find the optimal separating hyperplane between classes by focusing on the training data that are placed at the edge of the class descriptors. These training data are called support vectors. Training data other than support vectors are discarded. Thus, not only an optimal hyperplane is fitted, but also less training samples are effectively used (Tzotsos and Argialas, 2008). This method works very well for classes that are linearly separable. In the case that image classes are not linearly separable, the SVM maps the feature space into a higher dimensionality using kernels (Vapnik, 1998; Theodoridis and Koutroumbas, 2003) and then separates classes in that new feature space forming the support vectors.

Since the SVM classification method was initially designed for binary classification problems, a heuristic one-against-one strategy was employed for multiclass classification (Hsu and Lin, 2002). Many binary classifiers were applied for each pair of classes and for every object of the image and then a max-wins voting strategy determined the final classification of the object.

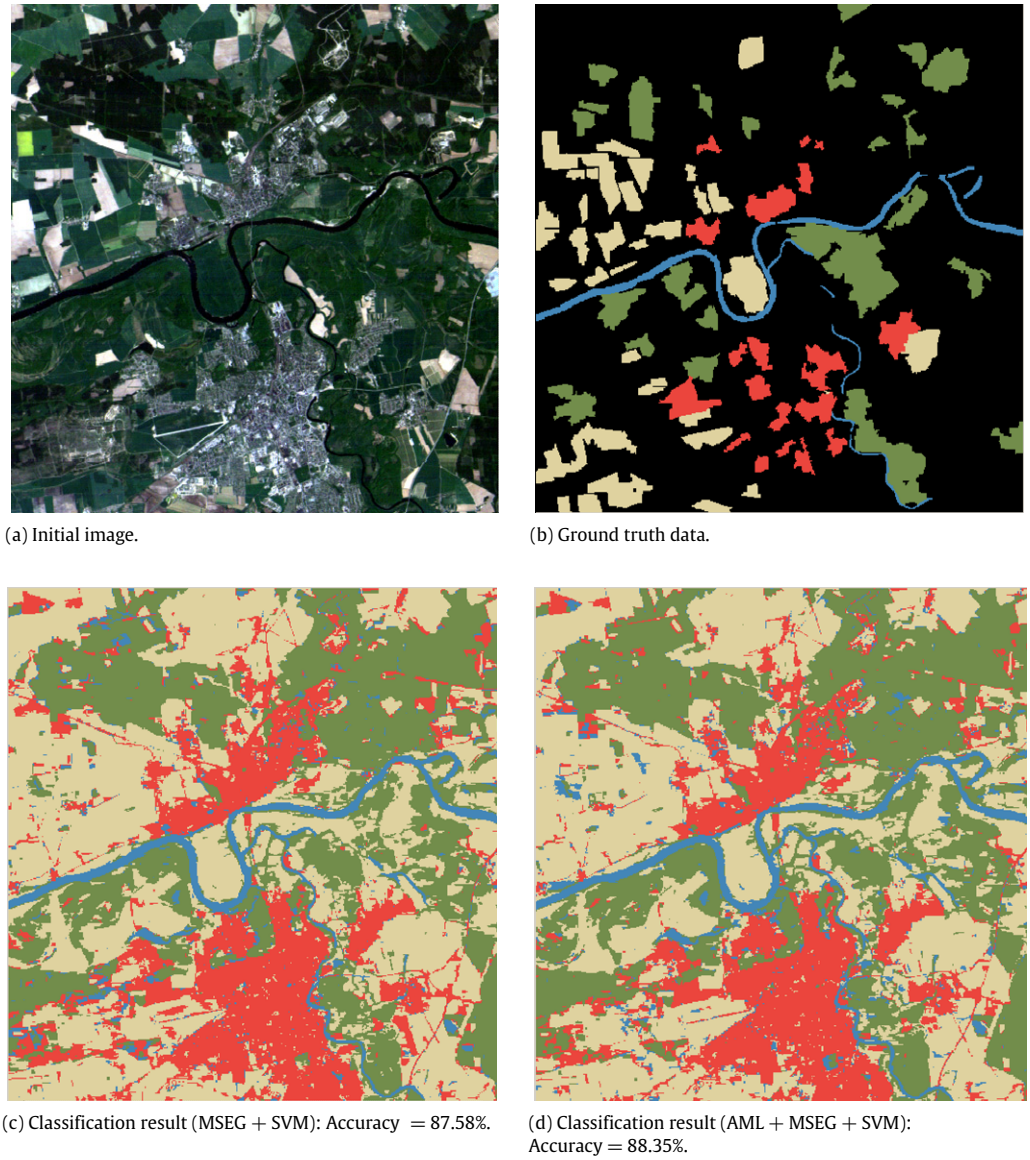

(a) Initial image.

(b) Ground truth data.

(c) Classification result (MSEG + SVM): Accuracy = 87.58%.

(d) Classification result (AML + MSEG + SVM): Accuracy = 88.35%.

Fig. 9. Original multispectral Landsat TM image (Dessau, Germany) and classification results with and without AML filtering. Blue: water bodies, yellow: grassland, green: woodland, red: impervious. (For interpretation of the references to colour in this figure legend, the reader is referred to the web version of this article.)

Since SVM is not a parameter-free method, the proper learning parameters had to be determined for each learning procedure. A cross-validation scheme was implemented. The training set was divided into several training subsets. Subsequently, some subsets were used for training and others for testing, while changing the training parameters. This process is iterative and the best parameters are determined after several iterations.

After determining the proper learning parameters with cross-validation, the training set was used to finally train the SVM. Then, using the one-against-one strategy, all image objects were classified and the class identification tag was applied to the object database. The final step of this procedure was the quantitative quality assessment, using ground truth data, for the formulation of confusion matrices and accuracy measurements.

To sum up, the initial dataset is simplified and a successive series of simplified images were constructed forming a nonlinear scale space. A multi-scale object representation was then computed from the scale space cubes without the tuning of any standard parameter (like shape, color, texture, etc.). Finally, the classifier based on the statistical properties of each object and their hierarchy associated each one with a land cover class.

4. Evaluation and discussion

As stated earlier, the objectives of the developed approach were (a) to formulate an advanced multi-scale object representation under an object-oriented framework, (b) to construct a processing system with the minimum tuning parameters and (c) to evaluate its performance regarding its qualitative and quantitative behaviour in various remote sensing datasets. In particular, of special interest are the very high spatial resolution data, which take classification methods to their limit, due to very high heterogeneity.

In Fig. 1, a comparison of linear and nonlinear scale-space representations is presented. The filtering result from a fine and a coarse scale is shown along with the corresponding image contours (isophotes) and segments. One can observe that linear approaches like Gaussian or down-sampling do not respect the edge information of the initial image and they degrade or blur the final image result. By observing the object contours after linear image simplification, it appears that a segmentation procedure may produce a smaller number of primitive image objects. This desired result, though, is not achieved for small objects of interest or image objects with strong edges. More specifically, in down-sampling methods, the boundary of the derived objects is less

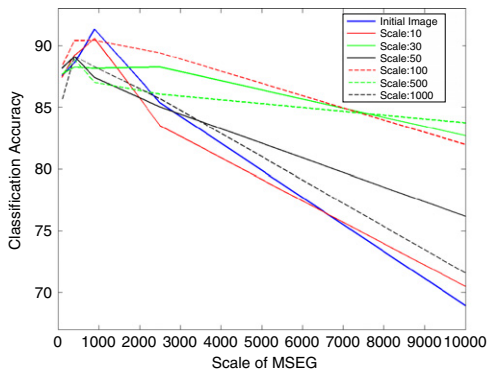

(a) ALM at Landsat TM image.

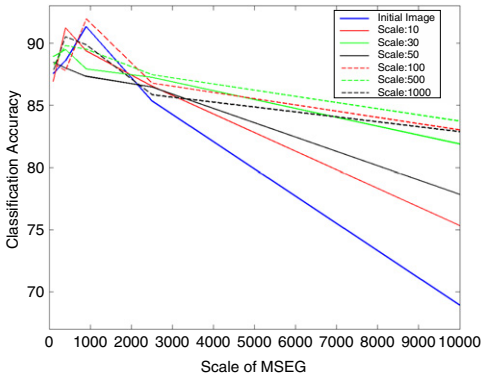

(b) AML at Landsat TM image.

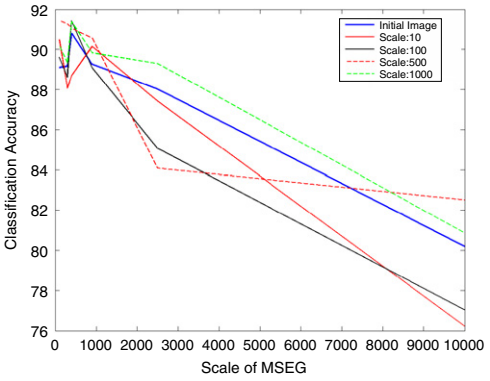

(c) ALM at Toposys aerial scan image.

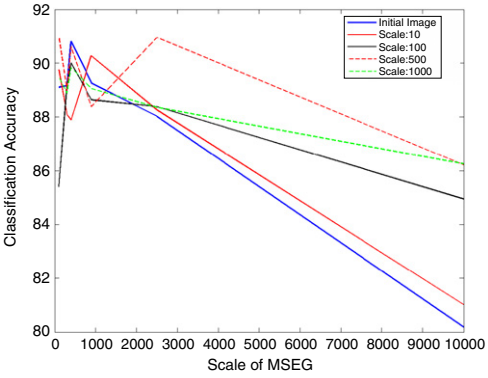

(d) AML at Toposys aerial scan image.

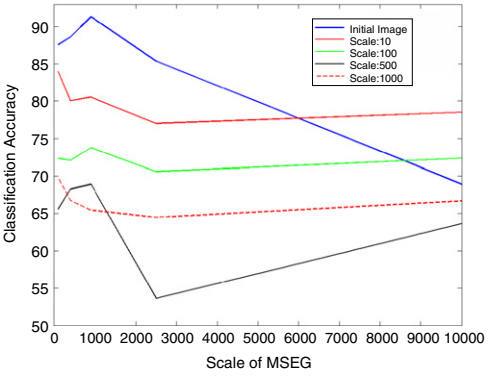

(e) Gaussian at Landsat TM image.

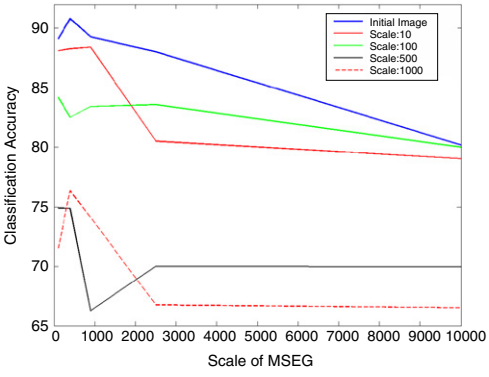

(f) Gaussian at Toposys aerial scan image.

Fig. 10. Sensitivity analysis regarding the accuracy of the classification result for different scales of filtering and segmentation.

smooth due to the pixel effect near the edges. The Gaussian filtering is mixing semantic objects after just a few scales of filtering.

On the other hand, anisotropic diffusion filtering (ALM) (Alvarez et al., 1992) preserves edge information even after a significant number of iterations (Fig. 1). Thus, the image semantics are protected from simplification. The main disadvantage of the ALM algorithm is that it alters the spectral signatures of image objects significantly which is not desired and acceptable for most remote sensing applications. This effect can be observed in Fig. 4, where a quantitative comparison of ALM and anisotropic morphological levelings takes place in the form of a spectral signature plot. The results were obtained from the application of nonlinear filtering on a TerraSAR-X dataset (Fig. 4). As shown in the plots, the ALM method creates new spectral values for the simplified pixels of the image that are far from the original spectral values. By contrast, the AML method used in this paper, simplifies the image while keeping the new values as close to the original as possible. In addition to edge preservation property, AML emerges as a superior method for scale-space representation. The simplified SAR images are shown in Fig. 4, while the evolution of the AML simplification across filtering scales is also shown.

In order to validate the developed algorithm's expirimental results and demonstrate its behaviour under several type of datasets and settings, two standard multi-scale segmentation techniques were employed: a multi-scale region-merging approach (MSEG) (Tzotsos and Argialas, 2006) and the coresponding one embeded in the eCognition software (Baatz and Schape, 2000).

4.1. Radar satellite imagery

The MSEG segmentation algorithm was first applied to the TerraSAR-X image. As shown in Fig. 5(a) and (b), the obtained primitive image objects are less in number after the simplification step.

(a) Original image.

(b) Ground truth data.

(c) SVM classification result (original image + MSEG). Accuracy = 89.1%.

(d) SVM classification result (AML scale 100 + MSEG). Accuracy = 90.16%.

(e) Nearest Neighbor classification result (original image). Accuracy = 86.72%.

(f) Nearest Neighbor classification result (AML scale 100). Accuracy = 87.35%.

Fig. 11. Original multispectral aerial scan image (Toposys©) and classification results with and without AML filtering. Green: vegetation, grey: asphalt materials, orange: tile roofs, white: bright roofs. (For interpretation of the references to colour in this figure legend, the reader is referred to the web version of this article.)

Moreover, the objects in (b) are more compact in shape and their boundaries are smoother than the ones in (a). It must be noted that both segmentation results were derived by the same segmentation parameters (scale parameter 100, color 0.8, shape 0.2, compactness 0.5 and smoothness 0.5). Furthermore, in (c) and (d), the same test was performed using the eCognition segmentation algorithm with similar results. Therefore, the nonlinear simplification addresses the over-segmentation problem and at the same time improves the shape of the resulting image objects by describing them more consistently with the real world objects.

4.2. Very high spatial resolution airborne imagery

The developed algorithm was also applied to an ultra-high spatial resolution dataset, with a pixel size of 5 cm from the DMC airborne digital scanner. The goal was to evaluate the behaviour of the introduced object-based framework for such a demanding task, i.e. classifying objects at such a large scale, processing a huge amount of information (hundreds of megabytes), construct thousands scale-space representations. This dataset (Figs. 1 and 3) shows that heterogeneity inside image objects of a specific thematic class can pose quite a challenge to any classification or segmentation algorithm available today.

In Fig. 3, steps from the simplification process are presented, while in Fig. 6 results from segmentation step and the construction of the multilevel object representations are shown. One can clearly observe that, without the tuning of any region merging parameters, the segmentation result is superior when using the AML filtering. In order to validate this observation with another region merging algorithm, the same experiments were performed with the eCognition segmentation algorithm. While the tiles of the roof on the initial image result into an over-segmented roof when using the standard merging processes, after the application of the AML simplification algorithm the tile heterogeneity is reduced and merging algorithms produce better outcomes. At the same time, those regions of the image which hold edge information are preserved (like dormer windows/roof windows). For those objects, the segmentation result does not change significantly, which is a desired behaviour. Once again, the smoothness of the resulting object boundaries is improved without changing the shape parameters of the segmentation algorithms.

As it is demonstrated in Fig. 7, similar conclusions can be derived when examining the behaviour of the developed algorithm at another region of the ultra-high spatial resolution dataset. It can be observed that segments in the car area/regions, where preserving the edge information is crucial in all filtering scales, the computed segments at finer and coarser scales did not change significantly. The same applies to objects that compose the street linings. On the other hand, street and vegetation segments show great improvement since the texture information is simplified in those regions of the image.

Table 1
Quantitative results regarding the classification accuracy for the multispectral LANDSAT TM image. The developed algorithm scored better in all cases, indicating that the combination of the advanced scale-space representation (AML) and the kernel classifier (SVM) outperform earlier approaches.

Classification accuracy without the AML (eCognition, Sc: 10)				
	Woodland	Grassland	Impervious	Waterbodies
Woodland	17 686	1 351	200	113
Grassland	1 524	14 033	119	4
Impervious	178	1 344	8563	6
Waterbodies	1 331	277	132	4 617
Overall accuracy: 87.22%				
Classification accuracy with the AML (eCognition, Sc: 10)				
Woodland	16 670	48	197	184
Grassland	3 528	15 624	179	21
Impervious	195	1 332	8577	11
Waterbodies	326	1	61	4 524
Overall accuracy: 88.18%				
Classification accuracy without the AML (MSEG, Sc: 100)				
	Woodland	Grassland	Impervious	Waterbodies
Woodland	16 479	3 551	352	337
Grassland	449	15 614	904	38
Impervious	189	263	8369	193
Waterbodies	111	2	3	4 624
Overall accuracy: 87.58%				
Classification accuracy with the AML (MSEG, Sc: 100)				
Woodland	16 661	3 264	298	496
Grassland	304	15 798	668	235
Impervious	93	2	1	4 644
Waterbodies	326	1	61	4 524
Overall accuracy: 88.35%				
Best classification result with the AML and MSEG at Sc: 900				
Woodland	15 864	39	0	1 883
Grassland	54	5 262	10	592
Impervious	0	107	8276	2 044
Waterbodies	151	635	154	35 419
Overall accuracy: 91.96%				

Table 2
Quantitative results regarding the classification accuracy for the high spatial resolution airborne multispectral TOPOSYS dataset. The developed algorithm scored better in all cases, indicating that the combination of the advanced scale-space representation (AML) and the kernel classifier (SVM) outperform earlier approaches.

Classification accuracy without the AML (eCognition, Sc: 10)				
	Vegetation	Tile roofs	Bright roofs	Asphalt like
Vegetation	15 597	1561	0	1 033
Tile roofs	33	3409	0	1 255
Bright roofs	0	118	8431	381
Asphalt like	2 156	830	1996	33 690
Overall accuracy: 86.72%				
Classification accuracy with the AML (eCognition, Sc: 10)				
Vegetation	15 437	1501	0	809
Tile roofs	22	3581	0	1 014
Bright roofs	0	17	8426	410
Asphalt like	2 327	819	2001	34 126
Overall accuracy: 87.35%				
Classification accuracy without the AML (MSEG, Sc: 100)				
	Vegetation	Tile roofs	Bright roofs	Asphalt like
Vegetation	15 731	0	0	2 055
Tile roofs	169	3072	81	2 596
Bright roofs	0	5	8333	2 089
Asphalt like	229	74	383	35 673
Overall accuracy: 89.10%				
Classification accuracy with the AML (MSEG, Sc: 100)				
Vegetation	15 603	285	0	1 898
Tile roofs	19	5454	9	436
Bright roofs	0	17	8355	2 055
Asphalt like	365	1496	358	34 140
Overall accuracy: 90.16%				
Best classification result with the AML and MSEG at Sc: 2500				
Vegetation	15 721	16	0	2 049
Tile roofs	61	5450	19	388
Bright roofs	0	2	8350	2 075
Asphalt like	120	217	317	35 705
Overall accuracy: 92.53%				

4.3. Multispectral remote sensing data

The next series of tests was performed on medium and high spatial resolution multispectral remote sensing data. For this, a Landsat TM image with pixel spatial resolution of 30 m was used, as well as an aerial scan with half a meter ground resolution and four spectral bands.

After a close look at the results (Fig. 8), one can observe the superior qualitative object representation acquired under the AML scale space filtering. This observation is validated by the classification results obtained using the same parameter settings when comparing with the ground truth data. In Fig. 9, the result of the classification comparison is demonstrated. Using exactly the same training samples in both cases, the SVM classification was improved as shown in Fig. 9 and Table 1. Moreover, the same test was performed using the nearest neighbor classifier. The overall classification accuracy was still improved, but could not match the accuracy of the advanced SVM classifier (Table 1).

At the same time, using the ground truth data, the proposed approach was tested in order to evaluate the obtained results. This result is presented in the form of a sensitivity analysis using the accuracy results from the SVM classifier (Fig. 10(a) and (b)). The best classification result obtained by the proposed approach for the Landsat image was at segmentation scale 900 and filtering scale 100 with an accuracy of 91.96% (Table 1).

The same evaluation test was performed on the multispectral image provided by Toposys. In Fig. 11, classification results are presented. The performance of the classifier was improved by the nonlinear scale-space filtering as shown also in Table 2. The sensitivity analysis performed for various segmentation and filtering scales is presented in Fig. 10(c) and (d). This test also included anisotropic filtering using ALM for comparison of results. The AML result is superior, especially on higher filtering scales, where the classification accuracy seems to be less sensitive to the scale variations.

Again, the developed framework was executed using the available ground truth data and the best classification result was found to be at segmentation scale 2500, AML scale 500 with overall accuracy of 92.53% (Table 2).

It can be observed that the classification through the AML scale-space representation has a more stable/consistent behaviour in both datasets, scoring higher accuracy rates at most filtering scales (Fig. 10). Although in approximately all cases the use of AML ameliorates significantly the classification accuracy, one can observe that from medium to coarser segmentation scales, the resulting improvement of the developed method is more than 10% compared to earlier efforts (eCognition, MSEG, etc.).

For further validation of the above results, the same number of tests was conducted on the multispectral datasets, after applying linear filtering instead of nonlinear filtering. As presented in Fig. 10(e) and (f), the SVM classification algorithm was performed on the same scales of the Gaussian filtered images, using the same training samples. Then, accuracy assessment was performed using the same ground truth data, obtaining new accuracy results. It can be observed (Fig. 10(e) and (f)) that the degradation of

the linearly filtered datasets caused a decrease of the maximum classification accuracy for each filtering scale and for both datasets. Also, while scale was increasing, the object-based classification process provided less accurate results.

As can be observed in Fig. 10, the application of the nonlinear filtering resulted to a more accurate classification for almost all filtering scales. Especially, for the AML filter the classification accuracy increased and it reached its peak (more than 90%) for the filtering scales of 100 and 500. In contrast, the application of the linear filtering in all cases and for almost all filtering scales impaired the accuracy of the classification (Fig. 10(e) and (f)).

5. Conclusions and future perspectives

A new object-based classification method was developed based on advanced scale-space representations, multilevel object representations and a support vector machine classifier. In contrast to previous efforts, we constructed the multilevel object representation based primarily on the advanced simplification procedure and not on the region merging process. The employed AML scale-space formulation was designed and which implicitly possesses a number of desired qualitative properties and thus eliminated the need for tuning several parameters during segmentation. The performed qualitative and quantitative evaluation reported that the developed algorithm outperformed previous efforts, both regarding the construction of the object representations and the classification results. The algorithm is stable, fast and can efficiently account for various classification tasks in various types of remote sensing data. Some of the topics for further research and development are solutions for object-specific extraction tasks based on the developed framework, incorporating unsupervised and knowledge-based classification approaches and optimizing the algorithm for real time applications.

Acknowledgements

The authors would like to thank the anonymous reviewers for their constructive comments and suggestions.

References

Alvarez, L., Lions, P.L., Morel, J.M., 1992. Image selective smoothing and edge detection by nonlinear diffusion. SIAM Journal on Numerical Analysis 29 (3), 845–866.

Aplin, P., Smith, G., 2008. Advances in object-based image classification. International Archives of the Photogrammetry, Remote Sensing and Spatial Information Sciences 37 (Part B7), 725–728.

Argialas, D., Harlow, C., 1990. Computational image interpretation models: an overview and a perspective. Photogrammetric Engineering & Remote Sensing 56 (6), 871–886.

Baatz, M., Schape, A., 2000. Multiresolution segmentation an optimization approach for high quality multi-scale image segmentation. In: Strobl, J., et al. (Eds.), Angewandte Geographische Informationsverarbeitung XII. Wichmann, Heidelberg, pp. 12–23.

Benz, U., Hofmann, P., Willhauck, G., Lingenfelder, I., Heynen, M., 2004. Multi-resolution, object-oriented fuzzy analysis of remote sensing data for GIS ready information. ISPRS Journal of Photogrammetry and Remote Sensing 58 (3–4), 239–258.

Blaschke, T., 2010. Object based image analysis for remote sensing. ISPRS Journal of Photogrammetry and Remote Sensing 65 (1), 2–16.

Blaschke, T., Burnett, C., Pekkarinen, A., 2004. Image segmentation methods for object-based analysis and classification. In: de Jong, S.M., van der Meer, F.D. (Eds.), Remote Sensing and Digital Image Analysis: Including the Spatial Domain. Kluwer Academic Publishers, pp. 211–236 (Chapter 12).

Blaschke, T., Hay, G., 2001. Object-oriented image analysis and scale-space: theory and methods for modeling and evaluating multi-scale landscape structure. International Archives of Photogrammetry and Remote Sensing 34 (Part 4/W5), 22–29.

Blaschke, T., Lang, S., Hay, G., 2008. Object Based Image Analysis—Spatial Concepts for Knowledge Driven Remote Sensing Applications. Springer, New York.

Camps-valls, G., Bruzzone, L., 2005. Kernel-based methods for hyperspectral image classification. IEEE Transactions on Geoscience and Remote Sensing 43 (6), 1351–1362.

Carleer, A., Debeir, O., Wolff, E., 2005. Assessment of very high spatial resolution satellite image segmentations. Photogrammetric Engineering & Remote Sensing 71 (11), 1285–1294.

Dragut, L., Schauppenlehner, T., Muhar, A., Strobl, J., Blaschke, T., 2009. Optimization of scale and parametrization for terrain segmentation: an application to soil–landscape modeling. Computers & Geosciences 35 (9), 1875–1883.

Duarte-Carvajalino, J., Castillo, P., Velez Reyes, M., 2007. Comparative study of semi-implicit schemes for nonlinear diffusion in hyperspectral imagery. IEEE Transactions on Image Processing 16 (5), 1303–1314.

Duarte Carvajalino, J., Sapiro, G., Velez Reyes, M., Castillo, P., 2008. Multiscale representation and segmentation of hyperspectral imagery using geometric partial differential equations and algebraic multigrid. IEEE Transactions on Geoscience and Remote Sensing 46 (8), 2418–2434.

Foody, G., Mathur, A., 2004. A relative evaluation of multiclass image classification by support vector machines. IEEE Transactions on Geoscience and Remote Sensing 42 (6), 1335–1343.

Hall, O., Hay, G.J., 2003. A multiscale object-specific approach to digital change detection. International Journal of Applied Earth Observation and Geoinformation 4 (4), 311–327.

Hay, G., Blaschke, T., Marceau, D., Bouchard, A., 2003. A comparison of three image–object methods for the multiscale analysis of landscape structure. ISPRS Journal of Photogrammetry and Remote Sensing 57 (5–6), 327–345.

Hay, G., Castilla, G., 2006. Object-based image analysis: strengths, weaknesses, opportunities and threats. International Archives of the Photogrammetry, Remote Sensing and Spatial Information Sciences 36 (Part 4/C42) (on CD-ROM).

Hay, G., Castilla, G., Wulder, M., Ruiz, J., 2005. An automated object-based approach for the multiscale image segmentation of forest scenes. International Journal of Applied Earth Observation and Geoinformation 7 (4), 339–359.

Hay, G.J., Dub, P., Bouchard, A., Marceau, D.J., 2002. A scale-space primer for exploring and quantifying complex landscapes. Ecological Modelling 153 (1–2), 27–49.

Hofmann, P., Strobl, J., Blaschke, T., 2008. A method for adapting global image segmentation methods to images of different resolutions. In: International Conference on Geographic Object-Based Image Analysis. International Archives of the Photogrammetry, Remote Sensing and Spatial Information Sciences 38 (Part 4/C1) (on CD-ROM).

Hsu, C.W., Lin, C.J., 2002. A comparison of methods for multiclass support vector machines. IEEE Transactions on Neural Networks 13 (2), 415–425.

Huang, C., Davis, L.S., Townshend, J.R.G., 2002. An assessment of support vector machines for land cover classification. International Journal of Remote Sensing 23 (4), 725–749.

Jimenez, L.O., Rivera-Medina, J.L., Rodriguez-Diaz, E., Arzuaga-Cruz, E., Ramirez-Velez, M., 2005. Integration of spatial and spectral information by means of unsupervised extraction and classification for homogenous objects applied to multispectral and hyperspectral data. IEEE Transactions on Geoscience and Remote Sensing 43 (4), 844–851.

Karantzalos, K., 2008. A 4D morphological scale space representation for hyperspectral imagery. International Archives of the Photogrammetry, Remote Sensing and Spatial Information Sciences 37 (Part B7), 127–132.

Karantzalos, K., Argialas, D., 2006. Improving edge detection and watershed segmentation with anisotropic diffusion and morphological levelings. International Journal of Remote Sensing 27 (24), 5427–5434.

Karantzalos, K., Argialas, D., Paragios, N., 2007. Comparing morphological levelings constrained by different markers. In: Banon, G., et al. (Eds.), Mathematical Morphology and its Applications to Signal and Image Processing (ISMM'07). pp. 113–124.

Koenderink, J., 1984. The structure of images. Biological Cybernetics 50 (5), 363–370.

Lennon, M., Mercier, G., Hubert-Moy, L., 2002. Classification of hyperspectral images with nonlinear filtering and support vector machines. In: IEEE International Geoscience and Remote Sensing Symposium. pp. 1670–1672.

Lindeberg, T., 1994. Scale-Space Theory in Computer Vision. Kluwer Academic Publishers, Dordrecht.

Liu, Y., Guo, Q., Kelly, M., 2008. A framework of region-based spatial relations for non-overlapping features and its application in object based image analysis. ISPRS Journal of Photogrammetry and Remote Sensing 63 (4), 461–475.

Matheron, G., 1997. Les nivellements. Technical Report. Centre de Morphologie Mathematique, France.

Melgani, F., Bruzzone, L., 2004. Classification of hyperspectral remote sensing images with support vector machines. IEEE Transactions on Geoscience and Remote Sensing 42 (8), 1778–1790.

Mercier, G., Lennon, M., 2003. Support vector machines for hyperspectral image classification with spectral-based kernels. In: IGARSS. Toulouse, France, 21–25 July (on CD-ROM).

Meyer, F., 1998. From connected operators to levelings. In: Heijmans, H., Roerdink, J. (Eds.), Mathematical Morphology and its Applications to Image and Signal Processing. Kluwer Academic, pp. 191–198.

Meyer, F., 2004. Levelings, image simplification filters for segmentation. International Journal of Mathematical Imaging and Vision 20 (1–2), 59–72.

Meyer, Y., Maragos, P., 2000. Nonlinear scale-space representation with morphological levelings. Journal of Visual Communication and Image Representation 11 (2), 245–265.

Neubert, M., Herold, H., Meinel, G., 2006. Evaluation of remote sensing image segmentation quality—further results and concepts. International Archives of the Photogrammetry, Remote Sensing and Spatial Information Sciences 34 (Part 4/C42), 6 p. (on CD-ROM).

Ouma, Y., Josaphat, S., Tateishi, R., 2008. Multiscale remote sensing data segmentation and post-segmentation change detection based on logical modeling: theoretical exposition and experimental results for forestland cover change analysis. Computers & Geosciences 34 (7), 715–737.

Pal, N.R., Pal, S.K., 1993. A review on image segmentation techniques. Pattern Recognition 26 (9), 1277–1294.

Paragios, N., Chen, Y., Faugeras, O., 2005. Handbook of Mathematical Models of Computer Vision. Springer-Verlag, New York.

Perona, P., Malik, J., 1990. Scale space and edge detection using anisotropic 683 diffusion. IEEE Transactions on Pattern Analysis and Machine Intelligence 12 (7), 629–639.

Plaza, A., Benediktsson, J.A., Boardman, J., Brazile, J., Bruzzone, L., Camps-valls, G., Chanussot, J., Fauvel, M., Gamba, P., Gualtieri, A., Marconcini, M., Tilton, J., Trianni, G., 2009. Recent advances in techniques for hyperspectral image processing. Remote Sensing of Environment 113 (Suppl. 1), S110–S122.

Serra, J., 2000. Connections for sets and functions. Fundamentale Informatica 41 (1–2), 147–186.

Stewart, S., Hay, G., Rosin, P., Wynn, T.J., 2004. Multiscale structure in sedimentary basins. Journal of Basin Research 16 (2), 183–197.

Theodoridis, S., Koutroumbas, K., 2003. Pattern Recognition, 2nd ed. Elsevier Academic Press, San Diego, California.

Tzotsos, A., Argialas, D., 2006. MSEG: a generic region-based multi-scale image segmentation algorithm for remote sensing imagery. In: Proceedings of ASPRS 2006 Annual Conference. Reno, Nevada, 1–5 May (on CD-ROM).

Tzotsos, A., Argialas, D., 2008. Support vector machine classification for object-based image analysis. In: Blaschke, T., Lang, S., Hay, G. (Eds.), Object Based Image Analysis—Spatial Concepts for Knowledge Driven Remote Sensing Applications. Springer, New York, pp. 663–679.

Tzotsos, A., Iosifidis, C., Argialas, D., 2008. A hybrid texture-based and region-based multi-scale image segmentation algorithm. In: Blaschke, T., Lang, S., Hay, G. (Eds.), Object Based Image Analysis—Spatial Concepts for Knowledge Driven Remote Sensing Applications. Springer, New York, pp. 221–237.

Vapnik, V., 1998. Statistical Learning Theory. John-Wiley and Sons, New York, USA.

Weickert, J., 1998. Anisotropic Diffusion in Image Processing. In: ECMI Series, Teubner-Verlag, Stuttgart, Germany.

Weickert, J., Ishikawa, S., Imiya, A., 1999. Linear scale-space has first been proposed in Japan. Journal of Mathematical Imaging and Vision 10 (3), 237–252.

Witkin, A., 1983. Scale-space filtering. In: International Joint Conference on Artificial Intelligence, vol. 8. Karlsruhe, Germany, pp. 1019–1021.

Zhou, W., Huang, G., Troy, A., Cadenasso, M., 2009. Object-based land cover classification of shaded areas in high spatial resolution imagery of urban areas: a comparison study. Remote Sensing of Environment 113 (8), 1769–1777.